Mechanisms of self-diffusion on Pt(110)

Lorensen, Henrik Qvist; Nørskov, Jens Kehlet; Jacobsen, Karsten Wedel

Published in:
Physical Review B

Link to article, DOI:
10.1103/PhysRevB.60.R5149

Publication date:
1999

Document Version
Publisher's PDF, also known as Version of record

PHYSICAL REVIEW B VOLUME 60, NUMBER 8 15 AUGUST 1999-II

Mechanisms of self-diffusion on Pt(110)

H. T. Lorensen, J. K. Nørskov, and K. W. Jacobsen
Center for Atomic-Scale Materials Physics and Physics Department, Technical University of Denmark, DK 2800 Lyngby, Denmark
(Received 8 February 1999)

The self-diffusion of Pt on the missing row reconstructed Pt(110) surface is discussed based on density functional calculations of activation energy barriers. Different competing diffusion mechanisms are considered and we show that several different diffusion paths along the reconstruction troughs are of relevance. The analysis leads to another interpretation of the recently observed double jumps at the Pt(110) surface. [S0163-1829(99)51732-3]

The field ion microscope (FIM) and the scanning tunneling microscope (STM) have made it possible to study diffusion processes at metal surfaces directly at the atomic level.[1,2] Recently, an STM was used to collect very detailed information in the form of ''STM movies'' of the self-diffusion on the Pt(110) surface.[2] From the data it was possible to extract adatom jump rates for both single atomic jumps where an adatom moves to a neighboring atomic site and for double jumps where the adatom is observed to move two sites away. In the following we discuss different possible diffusion mechanisms on the Pt(110) surface based on density functional total energy calculations. The observed double jumps have earlier been discussed in terms of dynamically correlated diffusion events[3] but here we give extensive density functional results showing that another mechanism is dominating.

The Pt(110) surface exhibits a missing row (MR) (1×2) reconstruction as shown in Fig. 1. The STM movies[2] show the Pt adatoms moving in the one-dimensional troughs formed by the reconstruction. The adatoms are found to occupy fourfold hollow sites in the reconstruction troughs and in the investigated temperature regime ($T=280$–380 K) isolated adatoms are never observed to cross from one trough to another. Based on a statistical analysis of the adatom trajectories it is possible to determine the jump rates for two different processes: the single jump which takes an adatom from a fourfold hollow site to a neighboring site, and the double jump which moves an adatom to the next-nearest site along the trough. An Arrhenius analysis of the jump rates show the temperature dependence of the rates k to be of the activated form $k=k_0\exp(-E/k_BT)$, where T denotes the temperature and E the activation energy. The activation energies are found to be[2] $E_s=(0.81\pm0.01)$ eV and $E_d=(0.89\pm0.06)$ eV for the single and double jumps, respectively. The corresponding prefactors are $k_{0,s}=10^{10.7\pm0.2}\ s^{-1}$ and $k_{0,d}=10^{10.9\pm0.8}\ s^{-1}$.

In the experiments, isolated adatoms are always observed in the fourfold hollow sites of the troughs due to the typical timescale of the imaging. It is therefore not possible to experimentally determine the detailed diffusion paths for the adatoms.

There are two natural diffusion paths for Pt adatoms in the troughs. One of the paths consists of direct motion of an adatom from a fourfold hollow site in a trough over a bridge site to a neighboring fourfold hollow site. This path which we shall refer to in the following as the ''direct'' path is indicated with line *A* in Fig. 1. The other diffusion path involves several steps. The sides of the reconstruction troughs can be viewed as small (111) facets with fcc and hcp adatom binding sites and it is possible for an adatom to move from a fourfold hollow site in a trough to a neighboring fourfold hollow site via the fcc and hcp sites on the facet as indicated by the path *B* in Fig. 1. We shall refer to this path as the ''facet'' path. These two paths were also investigated recently on the Au(110) surface with molecular dynamics on a semiempirical potential energy surface.[4]

We have investigated the energetics of the two diffusion paths using density functional theory[5] (DFT) with electronic exchange and correlation described within the generalized gradient approximation (GGA, PW91).[7] The surface is modeled by slabs of 5–9 Pt(110)-(1×2) layers. We use periodic boundary conditions in all three dimensions with a 2×2 surface unit cell and a separation between the slabs of at least 12 Å. Within the slabs a relaxed PW91 lattice parameter of 4.00 Å is used. The adatom is adsorbed on only one of the two slab surfaces, and the electrostatic potential is adjusted in the vaccum to compensate for dipoles on the surface introduced by the adatom. The ionic cores are described by ultrasoft

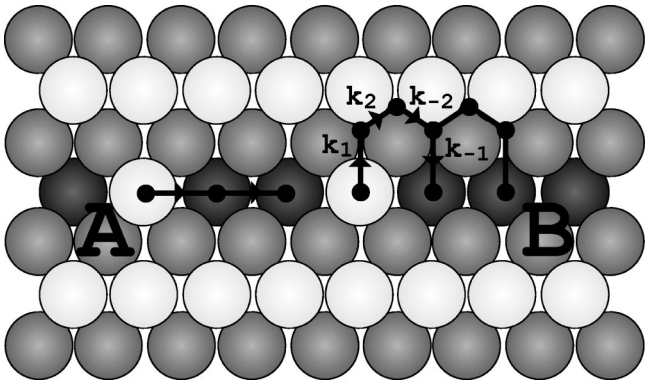

FIG. 1. Top view of the missing-row reconstructed (110) surface. Line *A* indicates the ''direct'' path between fourfold hollow sites. Line *B* indicate the ''facet'' path where hcp and fcc sites on the (111) microfacet are visited. Rates for the elementary jumps along the facet path are indicated: Index ''1'' for jumps from initial site to hcp site and index ''−1'' for the reverse direction. Index ''2'' indicates jumps from the hcp to the fcc site and index ''−2'' vice versa.

TABLE I. Diffusion barrier (in eV) for the direct path calculated for different numbers of layers. The barrier is converged with a nine layer slab.

Slab thickness	PW91	RPBE	LDA
5 layers	1.20	1.11	1.44
7 layers	1.08	0.99	1.29
9 layers	0.94	0.90	0.99
11 layers	0.93	0.90	0.99

pseudopotentials[6] generated within the PW91 approximation for exchange and correlation.[7] To ensure good transferability of the pseudopotentials, the nonlinear core correction[8] is employed using the core density beyond a cutoff $r_c^{Pt}=1.20$ Å and a second order polynomial for smaller r. The valence electron states are expanded on a basis of plane waves with kinetic energy up to 25 Ry. The first Brillouin zone is sampled on a $2\times4\times1$ Monkhorst-Pack grid.[9] The self-consistent density is found by iterative diagonalization of the Kohn-Sham Hamiltonian, Fermi population ($k_BT=0.1$ eV) of the Kohn-Sham states, and Pulay mixing of the electronic density.[10] All reported energies have been extrapolated to $T=0$. Convergence with respect to k-point sampling and energy cutoff has been checked to be better than 10 meV.

We have also performed non-self-consistent calculations of diffusion barriers with local-density approximation (LDA),[11] the Perdew-Burke-Ernzerhof scheme (PBE),[12] and revisions thereof (revPBE,[13] RPBE).[14] These calculations have been performed at the ionic geometry obtained with PW91 and also with the self-consistent PW91 electron density. The variational principle of density functional theory assures that small errors in the electron density will show up only to second order in the energy,[14,15] and since the ionic configurations we are interested in are stationary points of the potential energy surface, small deviations of the atomic positions should also only give small contributions to the energy. As a measure of this contribution, the activation energy for the direct path is also calculated self-consistently within the RPBE approximation (lattice parameter 4.02 Å). Compared to the non-self-consistent RPBE value, there is only a difference of 4 meV when the energy is calculated self-consistently.

As expected from their construction, the PBE results are quantitatively very similiar to the PW91 results. Likewise, the revPBE and RPBE are close to each other. At most, 10 meV differentiates PBE from PW91 and revPBE from RPBE. For this reason we will in the following focus on PW91 and RPBE values as well as values from LDA.

From calculated Hellmann-Feynman forces,[16] the ionic relaxation has been continued until a total residual force less than 0.05 eV/Å has been achieved.[17] For all the DFT calculations, the top three layers of the surface have been relaxed keeping deeper layers at bulk positions. For the 7 layer and 9 layer systems, only a small change in energy barriers came from relaxing layers below the first three layers (less than 20 meV for the 7 layer system with 5 layers relaxed). Table I illustrates the convergence with respect to slab thickness.

In Table II, energy differences with respect to the configuration of an adatom in a hollow site are listed. The table shows the energy at the transition state for the direct transition path and for the two lattice sites and the two saddle points along the facet path. The self-consistent PW91 values have been plotted in Fig. 2.

TABLE II. Site and transition state energies for the elementary diffusion steps for the direct path and the facet path (nine layer slabs). Energy values (in eV) are relative to a configuration with the adatom in the initial state.

Configuration	PW91	RPBE	LDA
Direct	0.94	0.90	0.99
Facet I	0.90	0.84	1.01
HCP	0.81	0.73	0.90
Facet II	0.94	0.84	1.09
FCC	0.67	0.58	0.79

The LDA gives barriers slightly higher than what is obtained with the GGA's. Within the two gradient corrected schemes, however, there is quite good agreement. The PW91 barriers are at most 0.10 eV larger than the RPBE barriers.

Comparing the transition state energies for the two competing diffusion paths we see that the barriers are close in value when calculated with the GGA schemes. With PW91 the direct path is as probable as the facet path, while with RPBE the facet path has a barrier which is 0.06 eV lower than for the direct path. With LDA the direct path is favored by 0.10 eV.

Before we turn to a comparison with the experimentally determined activation energies we note that the gradient corrections are known to lead to significant improvements over LDA for energetics of chemisorption systems. Among the gradient corrected schemes the revPBE/RPBE have been shown to give better agreement with experiment than PW91/PBE for adsorption energies of atoms and small molecules.[14] For the adatom self-diffusion considered here, both the PW91 and RPBE give good agreement with the experimentally obtained single jump activation energy of 0.81 eV. The remaining discrepancy can be ascribed to possible interaction effects between the adatoms due to the limited size of the surface unit cell and/or to the basic GGA approximation to

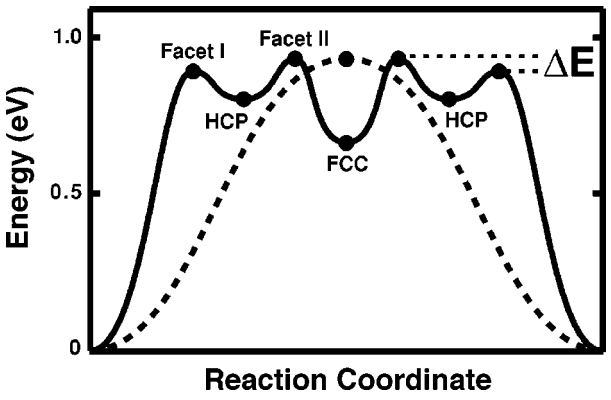

FIG. 2. PW91 energies along the path from one initial site to the neighboring. Calculated energies are indicated by bullets. The first jump on the facet path (full line) from the initial site to an hcp site is significantly higher than the other barriers involved in the facet diffusion. Consequently this jump will be the rate limiting step for the facet diffusion. ΔE indicates the barrier difference between continuing along the facet and falling down to an initial site.

the exhange-correlation energy and potential. Calculations of energy barriers for Pt self-diffusion on Pt(111) (Ref. 18) also show the GGA to overestimate the diffusion barrier on the (111) surface. In this study, the overestimation is smaller than what has previously been reported.

The GGA calculations indicate that the facet path could be the dominant one, and in the following we shall analyze the possibilities of single and multiple jumps along this path.

In Fig. 1 a schematic representation of the facet path is shown with labeling of the elementary steps in the path. As shown by Fig. 2 and the energies in Table II the barrier for the jump from the initial state to the hexagonally closed packed (HCP) site is significantly higher than other barriers involved. This jump will be the rate limiting step for the diffusion. In the time frame for jumps from one lattice site to the next, other elementary jumps can be assumed to be instantaneous.

In developing an expression for the rate for jumping m lattice sites, k_m, a sum over all possible paths on the facet must be made. For this reason, binomial coefficients enter into the final expression, which can be shown to be

$$k_{m-fold}=\frac{k_1 k_{-1}}{k_2+k_{-1}} F_m\left(\frac{1/2}{1+k_{-1}/k_2}\right). \tag{1}$$

The ''branching''-function F_m is

$$F_m(x)=\sum_{n=0}^{\infty}\binom{2n+m}{n}x^{2n+m}, \tag{2}$$

where the variable, x, is only dependent on the fraction between the rate for jumping down to the initial state (k_{-1}) and the rate for continuing along the facet (k_2).

The ratio between the rates for double jumps and single jumps now becomes

$$\frac{k_{2-fold}}{k_{1-fold}}=\frac{F_2\left(\frac{1/2}{1+k_{-1}/k_2}\right)}{F_1\left(\frac{1/2}{1+k_{-1}/k_2}\right)}\sim\frac{1}{2}e^{-(E_2-E_{-1})/k_BT}, \tag{3}$$

the exponential expression being the lowest order result in k_{-1}/k_2 assuming an Arrhenius expression for the rates k_{-1} and k_2 with the same prefactor: $k_{-1}=\nu e^{-E_{-1}/k_BT}$ and $k_2=\nu e^{-E_2/k_BT}$. From Table II the barrier difference $\Delta E=E_2-E_{-1}$ between continuing on the facet and falling down to a fourfold hollow site is 34, 4, and 76 meV for the PW91, RPBE, and LDA calculations, respectively.

In Fig. 3 the rates for single, double, and triple jumps based on expression (1) have been plotted in an Arrhenius fashion in a temperature range chosen to coincide with the range in[2] and using the self-consistent PW91 activation energies from Table II. Based on the assumption that the elementary steps in the diffusion have Arrhenius behavior, we see that both single and multiple jumps exhibit an Arrhenius dependence on temperature. From the Arrhenius plots in Fig. 3 the energy barriers can be calculated to be 0.92, 0.95, and 0.98 eV for the single, double, and triple jumps, respectively. The increase of barriers (0.03 eV) is close to the value (34 meV) that should be expected from the approximate expression (1) where only the lowest order term in k_{-1}/k_2 is included.

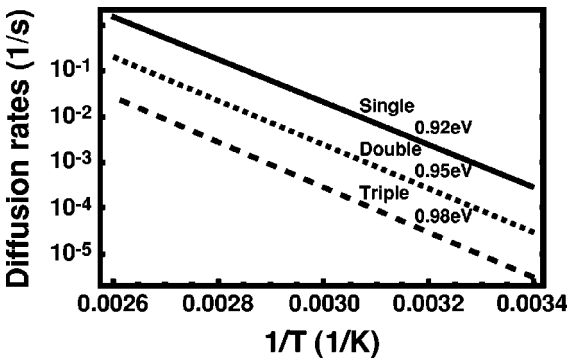

FIG. 3. Clear Arrhenius temperature dependence of diffusion rates for single, double, and triple jumps based on Eq. (1).

The calculated self-consistent PW91 results for the double jump rate compare quite favorably with the experimental observations.[2] The calculated rate is seen to approximately follow an Arrhenius behavior with an energy barrier which is about 34 meV higher than the one for single jumps. This is consistent with the experimentally determined difference in barrier heights of 80 ± 60 meV.[2] In Fig. 4 the fraction of double jumps to single jumps [Eq. (3)] is plotted vs the barrier difference $\Delta E=E_2-E_{-1}$ at a temperature of 350 K. For the self-consistent PW91 barrier difference the fraction is about 12%. Experimentally this fraction is of the order 5–10 %.[2]

As can be seen from Fig. 4, the number of double jumps depends rather sensitively on the barrier difference, especially at small values. If we take the RPBE values we therefore get far too many double jumps compared to experiment. However, as described above, the RPBE values are calculated non-self-consistently at the PW91 lattice parameter. It is possible that the numerical shift towards more double jumps are due to these errors in the non-self-consistent RPBE calculations.

It has been suggested that the explanation of the observed double jumps was due to dynamically correlated events.[3] However, we regard the explanation suggested here based on

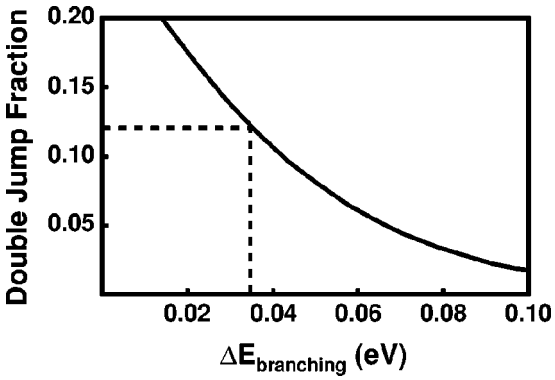

FIG. 4. Fraction of double jumps to single jumps at $T=350$ K as a function of barrier difference $\Delta E=E_2-E_{-1}$. In the range of barrier differences from the density functional theory (DFT) calculations, the fraction is comparable to the experimentally observed value.

the facet path mechanism more likely for the following reasons: The earlier investigation was based on the effective medium theory (EMT) (Ref. 19) potential which, just like LDA, does not favor the facet path.[20] The self-consistent GGA results presented here clearly show the relevance of this path. The dynamically correlated double jumps were shown to also approximately obey an Arrhenius behavior with an increased activation energy of about 0.12 eV obtained with the EMT potential. However, the double jump prefactor is not the same as for the single jumps and in the experimentally relevant temperature regime it is approximately an order of magnitude smaller (see for example, Fig. 3 of Ref. 3). The number of double jumps due to dynamically correlated events must therefore be expected to be less than 1% of the single jumps.

In conclusion, we have shown that apart from the usual ''direct'' diffusion path a ''facet'' path may also be important for the diffusion of Pt adatoms on the missing row reconstructed Pt(110) surface. This opens up for an explanation of the observed double jumps in terms of a series of elementary diffusion steps on the facet rather than a correlated diffusion process along the ''direct'' path.

Stimulating discussions with Flemming Besenbacher and Sebastian Horch are gratefully acknowledged. The present work was in part financed by The Danish Research Councils through grant No. 9501775. The Center for Atomic-Scale Materials Physics is sponsored by the Danish National Research Foundation.

[1] G. Ehrlich, Surf. Sci. **246**, 1 (1991); G. Kellogg, Surf. Sci. Rep. **21**, 1 (1994).

[2] T. R. Linderoth, S. Horch, E. Lægsgaard, I. Stensgaard, and F. Besenbacher, Phys. Rev. Lett. **78**, 4978 (1997).

[3] J. Jacobsen, K. W. Jacobsen, and J. Sethna, Phys. Rev. Lett. **79**, 2843 (1997).

[4] F. Montalenti and R. Ferrando, Phys. Rev. B **58**, 3617 (1998).

[5] P. Hohenberg and W. Kohn, Phys. Rev. B **136**, 864 (1964); W. Kohn and L. Sham, Phys. Rev. A **140**, 1133 (1965).

[6] D. H. Vanderbilt, Phys. Rev. B **41**, 7892 (1990).

[7] J. P. Perdew, J. A. Chevary, S. H. Vosko, K. A. Jackson, M. R. Pederson, D. J. Singh, and C. Fiolhais, Phys. Rev. B **46**, 6671 (1992).

[8] S. G. Louie, S. Froyen, and M. L. Cohen, Phys. Rev. B **26**, 1738 (1982).

[9] H. J. Monkhorst and J. D. Pack, Phys. Rev. B **13**, 5188 (1976).

[10] G. Kresse and J. Furthmüller, Comput. Mater. Sci. **6**, 15 (1996).

[11] D. M. Ceperley and B. J. Alder, Phys. Rev. Lett. **45**, 566 (1980).

[12] J. P. Perdew, K. Burke, and M. Ernzerhof, Phys. Rev. Lett. **77**, 3865 (1996).

[13] Y. Zhang and W. Yang, Phys. Rev. Lett. **80**, 890 (1998).

[14] B. Hammer, L. B. Hansen, and J. K. Nørskov, Phys. Rev. B **59**, 7413 (1999).

[15] B. Hammer, K. W. Jacobsen, and J. K. Nørskov, Phys. Rev. Lett. **70**, 3971 (1993).

[16] J. Ihm, A. Zunger, and M. L. Cohen, J. Phys. C **12**, 4409 (1979).

[17] The residual force is calculated as $(\Sigma_i|\overline{f_i}|^2)^{1/2}$, where the sum is over the forces, $\overline{f_i}$, on all relaxed atoms.

[18] P. J. Feibelman, J. S. Nelson, and G. L. Kellogg, Phys. Rev. B **49**, 10 548 (1994); J. J. Mortensen, B. Hammer, O. H. Nielsen, K. W. Jacobsen, and J. K. Nørskov, *The 18th Taniguchi Symposium on Elementary Processes in Excitations and Reactions on Solid Surfaces*, edited by A. Okiji (Springer-Verlag, Berlin, 1996); G. Boisvert, L. J. Lewis, and M. Scheffler, Phys. Rev. B **57**, 1881 (1998).

[19] K. W. Jacobsen, P. Stoltze, and J. K. Nørskov, Surf. Sci. **366**, 394 (1996).

[20] The EMT barrier for the ''direct'' path is 0.47 eV. This should be compared to the EMT ''facet'' path barriers of 0.58 eV and 0.66 eV for the first and second barrier, respectively.